

Drug Delivery | *Hot Paper*

Double Sequential Encrypted Targeting Sequence: A New Concept for Bone Cancer Treatment

Gonzalo Villaverde, Valentina Nairi, Alejandro Baeza,* and María Vallet-Regí*^[a]

In memory of José Barluenga Mur



Abstract: The selective transportation of therapeutic agents to tumoral cells is usually achieved by their conjugation with targeting moieties able to recognize these cells. Unfortunately, simple and static targeting systems usually show a lack in selectivity. Herein, a double sequential encrypted targeting system is proposed as a stimuli-responsive targeting analogue for selectivity enhancement. The system is able to recognize diseased bone tissue in the first place, and once there, a hidden secondary targeting group is activated by the presence of an enzyme overproduced in the malignant tissue (cathepsin K), thereby triggering the recognition of diseased cells. Transporting the cell targeting agent in a hidden conformation that contains a high selective tissular primary targeting, could avoid not only its binding to similar cell receptors but also the apparition of the binding-site barrier effect, which can enhance the penetration of the therapeutic agent within the affected zone. This strategy could be applied not only to conjugate drugs but also to drug-loaded nanocarriers to improve the efficiency for bone cancer treatments.

The lack in selectivity of cytotoxic drugs results in their ineffective delivery to tumor tissues, which strongly reduces efficacy and causes the apparition of systemic toxicity in usual cancer treatments.^[1] Moreover, even if the drug reaches the tumor area, it will face a complex scenario. A solid tumor is an extraordinary heterogeneous tissue formed by a myriad of different malignant, harmless, even supportive cells, which play different roles in tumor progression.^[2] Therefore, it is necessary to design smart therapeutic agents with the ability to distinguish between healthy and tumor cells in order to enhance their efficiency through the concentration of their cytotoxic capacity exclusively in malignant cells. One of the promising alternatives for improving the selectivity of chemotherapy is the covalent conjugation of vectorization moieties or targeting systems directly on the surface of drug-loaded nanocarriers,^[3] with both inorganic^[4,5] and organic nature,^[6,7] as well as to free drugs^[8] generating vectorized drug conjugates. A wide variety of targeting systems, from big biomolecules like antibodies,^[9] lipoproteins,^[10] or oligonucleotide sequences^[11] to small molecules such as vitamins,^[12] sugars,^[13] or synthetic molecules,^[14] are known. These moieties are characterized by their capacity to recognize and specifically bind to membrane cell receptors which are only, or mainly, expressed by tumor cells. Unfortun-

nately, the use of targeting moieties is not free of drawbacks, for example unwanted off-target effects caused by the protein corona,^[15] non-desired modifications of the ligand during the conjugation process,^[16] or cross interactions between the targeting group and cell receptors expressed in healthy cells. On the other hand, a strong binding affinity between the vectorization motif and its cell receptor severely hampers the penetration of the therapeutic agent within the tumor. The apparition of this well-known effect, called binding-site barrier, is common in both drug conjugates^[17] and targeted nanoparticles^[18] and compromises the efficacy of the therapy by accumulation of targeted systems mainly in the tumor periphery, inducing only weak local effects.

Hierarchical targeting has been recently proposed as a novel strategy able to overcome these limitations in the case of nanometric carriers.^[19] However, using shielded targeting agents in this context makes the EPR (enhanced permeability and retention)^[20,21] effect as solely responsible for nanocarrier accumulation in tumor tissues.^[22] Therefore, the achieved gain regarding lower cross interactions and higher penetration could be counteracted by the lower amount of nanocarriers that reach the diseased zone. Additionally, this approach is hardly adaptable to the direct conjugation with small drugs, since these therapeutic agents do not present an EPR effect as a consequence of their smaller size.

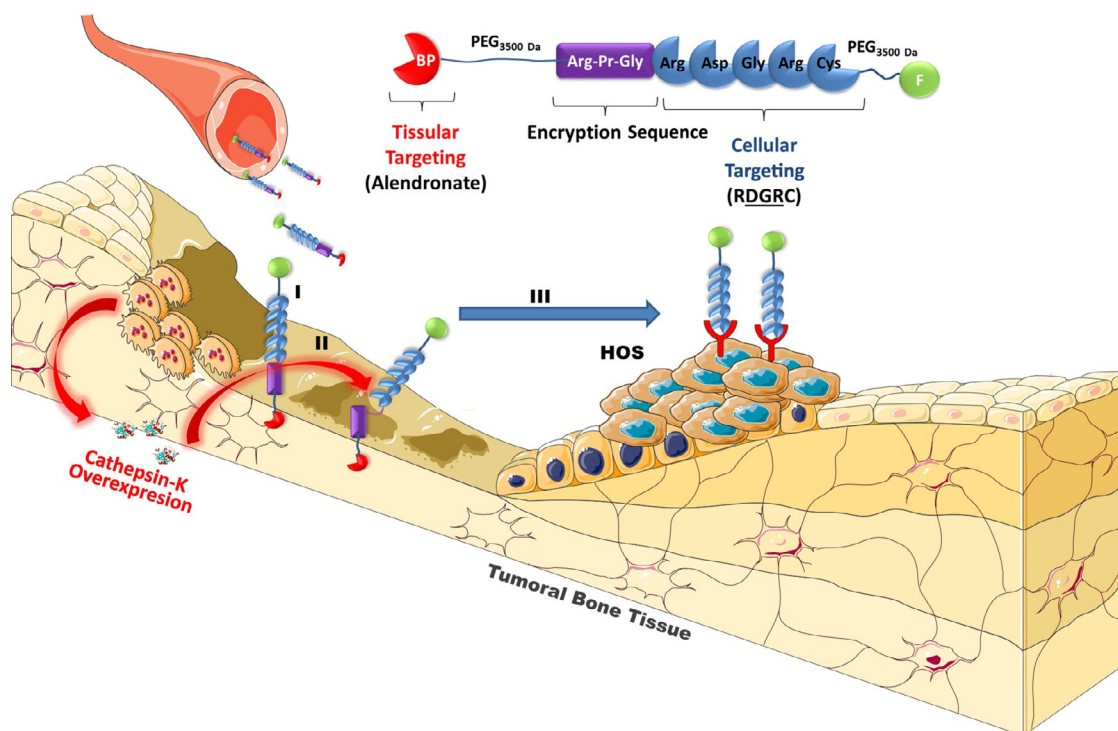
Herein, we propose a novel approach equally applicable to both drug conjugates and nanocarriers. This concept is based on a double sequential encrypted targeting system (DSETS) capable to combine tissular and cellular targeting following an activatable cascade mechanism. As proof of concept, we have focused on bone tumors. Thereby, we have chosen an uncovered primary tissue targeting agent, bisphosphonate (BP), that is specific for exposed diseased bone tissue, and a secondary hidden cellular targeting moiety of the "RGD type". The peptide has been encrypted inside an oligopeptide sequence RPGRDGRGRC (Arg-Pr-Gly-Arg-Asp-Gly-Arg-Cys) and has been sterically covered with a polyethyleneglycol 3500 Da (PEG) moiety, making it more inert in presence of its receptors. Then, the RGD pattern becomes exposed only in the presence of elevated concentrations of cathepsin K (CK), a characteristic condition in bone tissues with high osteoclast activity such as many primary and metastatic bone tumors^[23,24] (Scheme 1). This novel targeting moiety is based on the combination of two widely employed targeting agents; alendronate^[25] (ALN) and the RGD tripeptide^[26,27]. Alendronate shows a high affinity for hydroxyapatite and, therefore, this molecule strongly binds to the mineral part of bone tissues.^[28]

On the other hand, the RGD pattern is a well-known sequence that binds to α , β -integrin and Neuropilin (NRP)-1 receptors, which are usually overexpressed in many tumoral cell lines and also in tumoral blood vessels.^[29]

However, integrin receptors are also present in many healthy cells and, therefore, the direct conjugation of RGD sequences on the transported species could misdirect the therapeutic cargo to unwanted locations. The combination of both vectorization capacities (tissular and cellular targeting) converts this modular targeting system into a promising prototype for deliv-

[a] Dr. G. Villaverde, V. Nairi, Dr. A. Baeza, Prof. M. Vallet-Regí
Depto. Química Inorgánica y Bioinorgánica, Facultad de Farmacia
Universidad Complutense de Madrid. Plaza Ramon y Cajal s/n.
Instituto de Investigación Sanitaria Hospital 12 de Octubre i + 12 j
Centro de Investigación Biomédica en Red de Bioingeniería,
Biomateriales y Nanomedicina (CIBER-BBN), Madrid (Spain)
E-mail: abaezaga@ucm.es
vallet@ucm.es

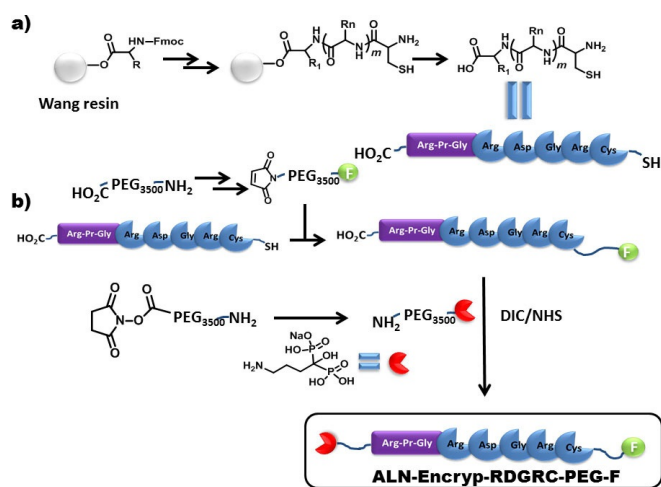
Supporting information for this article, containing synthetic procedures, NMR and MALDI-TOF/TOF spectra, cell culture protocols, and flow cytometry measurements, can be found under: <http://dx.doi.org/10.1002/chem.201605947>.



Scheme 1. Mode of action of the double sequential targeting system in osteosarcoma diseased bone. I) Bone targeting of BP (bisphosphonate) to HA (hydroxyapatite). II) Cathepsin K (CK) induced peptide proteolysis. III) RGD peptide recognition by HOS (human osteosarcoma) cell wall and subsequent internalization.

ering therapeutic agents to bone tumors. For affording the targeting device, the first step was the synthesis of the polypeptide strand, which was made using solid-phase chemistry starting from a Fmoc-Arg(Pbf)-Wang resin (see the Supporting Information for the detailed protocol).

Following the typical Fmoc-deprotection and HBTU/HOBT-mediated carboxylic acid activation steps, each individual amino acid was added to the peptide strand (Scheme 2a). The tripeptide Arg-Pr-Gly motif was introduced in the sequence for providing selective responsivity to CK. This enzyme performs



Scheme 2. Synthetic pathway affording the fluorescent dual-targeting moiety.

the proteolysis of collagen I, catalyzing almost exclusively the rupture of the amide bond present in the helix after a Pr-Gly motif.^[30,31]

To evaluate the sensitivity and selectivity against CK, a small amount of the peptide strand (10 mg) was exposed to an acidic solution of this enzyme (pH 5) for 2 h at 37 °C, replicating osteoclast lacuna conditions, whereas the other batch was only exposed to mild acidic medium. After the isolation process, the resulting crude products were analyzed by matrix-assisted laser desorption/ionization (MALDI) time-of-flight/time-of-flight (TOF/TOF) spectrometry. As expected, when the peptide was exposed to CK, Arg-Asp-Gly-Arg-Cys was the mayor product, which corresponds to an amide bond rupture after glycine in Pr-Gly (Figure S10 in the Supporting Information). This result confirms that CK induces the responsive behavior of the peptide strand in comparison to its stability showed under enzyme-free conditions. A fluorescently labeled polyethyleneglycol (F-PEG) was employed as the therapeutic cargo model. This polymeric strand mimics the role of the nanometric drug-loaded carrier or therapeutic macromolecule allowing an easy visualization and quantification of the system internalization within malignant cells, as it has been reported elsewhere.^[32] F-PEG-Maleimide was attached to the cysteine end through thiol-ene reaction. Alendronate was conjugated via carbodiimide chemistry to the carboxylic acid end of a bifunctional HO₂C-PEG-NH₂ chain of a molecular weight of 3500 Da to shield the cellular targeting moiety more properly. Finally, this system was attached to the fluorescent peptide strand using again a carbodiimide as carboxylic acid activator (Scheme 2b).

Once the system was prepared, its performance was evaluated step by step. First, its capacity to bind to apatite was tested by incubating the complete system in the presence of pure hydroxyapatite discs (HA) in PBS (pH 7.4) at 37 °C for 8 h to simulate body fluid conditions. The peptide sequence without the PEG-alendronate moiety was employed as control. After completion of the incubation time, the discs were thoroughly washed with buffer to eliminate physically adsorbed systems and their presence was determined by fluorescence microscopy. As expected, the peptides without alendronate were not able to bind to the surface of the HA discs, whereas the peptides with alendronate were strongly retained on the HA surfaces (Figure 1 a). Further, the binding capacity was also evaluated in the presence of Ca^{2+} at a concentration of 2.5 mM, which is naturally present in the bone tissue surroundings. HA discs with the complete system were incubated in the presence of physiological concentrations of Ca^{2+} , showing the retention of the fluorescence in a similar amount than controls without Ca^{2+} (Figure 1 b). As shown in Figure 1 b, it was necessary to double this concentration to releasing a significant amount of the targeting moiety.

To prove that the binding capacity of the complete system was due to the complexation of alendronate on the HA surface, competition experiments with free alendronate were carried out. As shown in Figure 1 c, the systems ability to be retained on the HA surface decreased when the alendronate concentration was higher, due to free alendronate gradually replacing the complete targeting device from the surface. In all experiments, the targeting system release was confirmed by fluorescence measurements of the solutions before and after

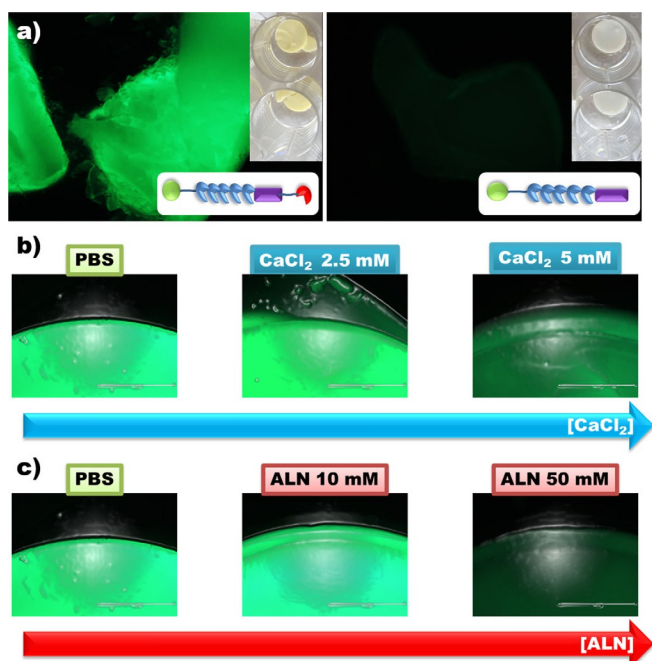


Figure 1. a) Fluorescence microscopy of HA discs exposed to the targeting molecule with and without PEG-ALN (polyethyleneglycol-alendronate). Fluorescence microscopy of HA discs exposed to the complete targeting molecule in the presence of different concentrations of b) Ca^{2+} and c) free alendronate.

the alendronate exposition (Graphic S1 in the Supporting Information). In sight of these evidences, the active primary targeting moiety inside the complete system showed a good performance under close-to-reality conditions for vectorization to the diseased bone.

The next step was to evaluate the performance of the hidden secondary targeting sequence. For this aim, human osteosarcoma (HOS) cells were chosen as tumoral cell model because they usually overexpress $\alpha_v\beta_3$ -integrin^[33] and (NRP)-1 receptors,^[34] which interact with the RGD pattern. Further, osteosarcoma is one of the most common non-hematologic neoplasm that affects bone tissues.^[35] The capacity to hide the secondary targeting was evaluated by exposing HOS cells to a fixed concentration of the complete system ($10 \mu\text{g mL}^{-1}$) for 2 h. The same protocol was carried out employing a fluorescent PEG strand (F-PEG) as negative control and a fluorescent PEG strand decorated with CRGDR as positive control (F-PEG-CRGDR). The percentage of cells that internalize the fluorescent strands in each case was measured using flow cytometry. Almost 20% of HOS cells internalize the fragment that contains the unshielded RGD pattern in comparison with only 8% that engulf the fluorescent PEG, which confirms that the RGD sequence enhances the internalization within malignant cells (Figure 2). Interestingly, the targeting uptake was only 12% (all data normalized with control) when the complete system containing the shield pattern was employed, which corresponds to a decrease of the targeting internalization of around 40%. Thus, these results point out a good performance of both encryption and cell targeting capacity of the hybrid strand.

Finally, the complete system was tested employing a “bone/culture in vitro model”. In this model, HA discs were previously incubated with a PBS solution that contains $300 \mu\text{g mL}^{-1}$ of the complete system. After 8 h, the discs were thoroughly washed with buffer to remove physisorbed peptides. Once washed, the discs were placed on the upper sheet of transwells and the cells were cultured on the bottom. Then, the wells were incubated in mild-acidic media for 2 h, three with addition of CK and three without. After the incubation time, the HA discs were removed and the cell cultures were washed with PBS and incubated with medium for another 24 h.

The targeting internalization in each well was analyzed by flow cytometry showing that, in the samples to which cathepsin K was added, around 90% of the cells showed fluorescence, which indicates the internalization of the labeled peptide. On the contrary, in the wells incubated without CK, only around 10% of the cells exhibited fluorescence. The presence of the peptide in each disc was observed by fluorescence microscopy. The discs that were treated with incubated proteolytic enzyme lost all fluorescence, whereas those without the enzyme almost completely retained their fluorescence (Figure 3).

Osteosarcoma has been chosen as proof of concept of a common solid tumor and therefore, the primary and secondary targeting groups were selected accordingly. But it is worth noting that this strategy could be easily adapted to different tumors that affect different organs or tissues. In conclusion, encrypted targeting agents would avoid the misdirection

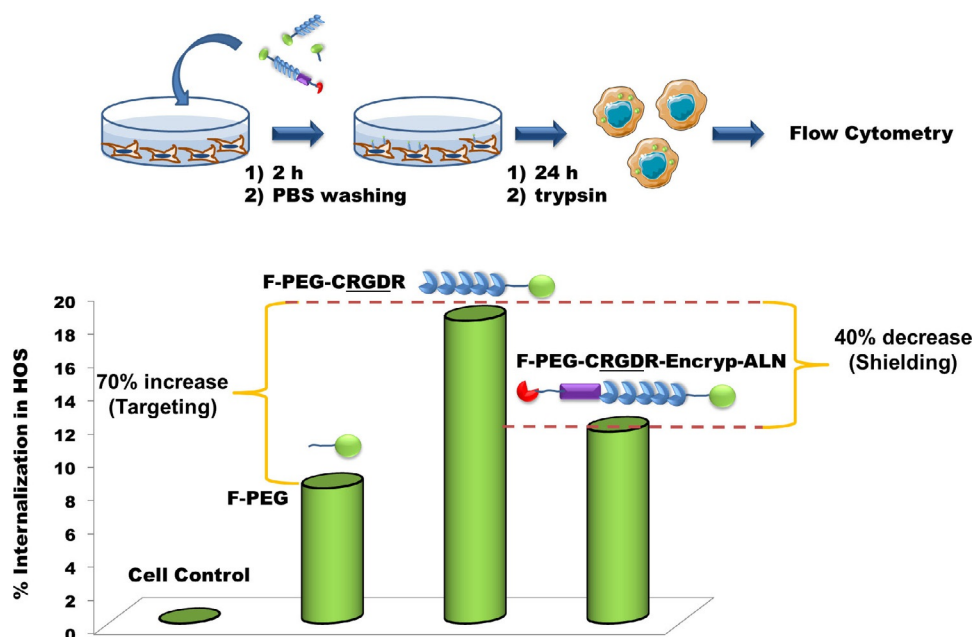


Figure 2. Studies of the internalization capacity of F-PEG (fluorescently labeled PEG), F-PEG-CRGDR and F-PEG-CRGDR-Encryp-ALN in HOS. Error data and statistical analysis can be found in the Supporting Information. CRGDR = Cys-Arg-Gly-Asp-Arg. CRGDR-Encryp = Cys-Arg-Gly-Asp-Arg-Gly-Pro-Arg.

of the transported species to other tissues, thereby reducing the apparition of side effects or systemic toxicity. Additionally, the primary targeting group located at the end of the full system provides the guiding capacity to the affected tissue.

This novel targeting system represents a new approach for the selectivity enhancement in drug delivery processes and could be applied for several types of drug conjugates, drug-loaded nanocarriers, or imaging agents, increasing the available arsenal in the fight against tumors.

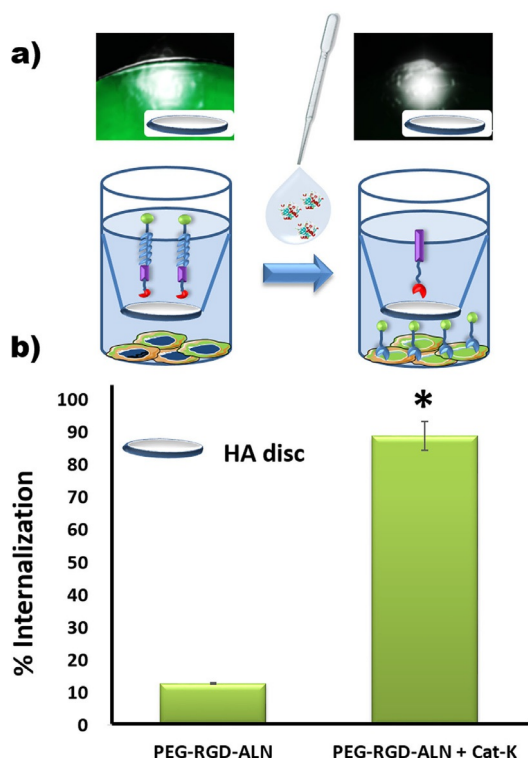


Figure 3. Cat-K responsive behavior of F-PEG-CRGDR-Encryp-ALN in HOS. a) Fluorescence microscopy of the HA discs with F-PEG-CRGDR-Encryp-ALN before and after Cat-K treatment. b) Percentage of cells that have engulfed the fluorescent label. * $P < 0.01$.

Acknowledgements

This work was supported by the European Research Council (Advanced Grant VERDI; ERC-2015-AdG Proposal No. 694160) and the project MAT2015-64831-R. The authors want to thank Prof. Maura Monduzzi for her support along this work. For the elaboration of Figures and Schemes, some templates from <http://www.servier.com/Powerpoint-image-bank> have been used.

Conflict of interest

The authors declare no conflict of interest.

Keywords: cancer · drug delivery · dual targeting · encrypted peptide · stimuli-responsive targeting

- [1] K. D. Miller, R. L. Siegel, C. C. Lin, A. B. Mariotto, J. L. Kramer, J. H. Rowland, K. D. Stein, R. Alteri, A. Jemal, *CA. Cancer J. Clin.* **2016**, *66*, 271–289.
- [2] M. Egeblad, E. S. Nakasone, Z. Werb, *Dev. Cell* **2010**, *18*, 884–901.
- [3] R. Bazak, M. Hourri, S. El Achy, S. Kamel, T. Refaat, *J. Cancer Res. Clin. Oncol.* **2015**, *141*, 769–784.
- [4] M. Vallet-Regí, A. Rámila, R. P. del Real, J. Pérez-Pariente, *Chem. Mater.* **2001**, *13*, 308–311.
- [5] M. Vallet-Regí, F. Balas, D. Arcos, *Angew. Chem. Int. Ed. Engl.* **2007**, *46*, 7548–58.

- [6] M. Talelli, M. Barz, C. J. F. Rijcken, F. Kiessling, W. E. Hennink, T. Lammers, *Nano Today* **2015**, *10*, 93–117.
- [7] M. C. Parrott, J. C. Luft, J. D. Byrne, J. H. Fain, M. E. Napier, J. M. DeSimone, *J. Am. Chem. Soc.* **2010**, *132*, 17928–17932.
- [8] E. L. Sievers, P. D. Senter, *Annu. Rev. Med.* **2013**, *64*, 15–29.
- [9] Q. Dai, Y. Yan, C. Ang, K. Kempe, M. M. J. Kamphuis, S. J. Dodds, F. Caruso, *ACS Nano* **2015**, *9*, 2876–2885.
- [10] S. Lara, F. Alnasser, E. Polo, D. Garry, M. C. Lo Giudice, D. R. Hristov, L. Rocks, A. Salvati, Y. Yan, K. A. Dawson, *ACS Nano* **2017**, *11*, 1884–1893.
- [11] Y. Lao, K. K. L. Phua, K. W. Leong, *ACS Nano* **2015**, *9*, 2235–2254.
- [12] H. Elnakat, M. Ratnam, *Adv. Drug Deliv. Rev.* **2004**, *56*, 1067–1084.
- [13] H. Nguyen, P. Katavic, N. A. H. Bashah, V. Ferro, *ChemistrySelect* **2016**, *1*, 31–35.
- [14] G. Villaverde, A. Baeza, G. J. Melen, A. Alfranca, M. Ramirez, M. Vallet-Regí, *J. Mater. Chem. B* **2015**, *3*, 4831–4842.
- [15] A. Salvati, A. S. Pitek, M. P. Monopoli, K. Prapainop, F. B. Bombelli, D. R. Hristov, P. M. Kelly, C. Åberg, E. Mahon, K. A. Dawson, *Nat. Nanotechnol.* **2013**, *8*, 137–143.
- [16] L. M. Herda, D. R. Hristov, M. C. Lo Giudice, E. Polo, K. A. Dawson, *J. Am. Chem. Soc.* **2017**, *139*, 111–114.
- [17] R. Bakhtiar, *Biotechnol. Lett.* **2016**, *38*, 1655.
- [18] T. Lammers, F. Kiessling, W. E. Hennink, G. Storm, *J. Control. Release* **2012**, *161*, 175–187.
- [19] S. Wang, P. Huang, X. Chen, *Adv. Mater.* **2016**, *28*, 7340–7364.
- [20] J. Fang, H. Nakamura, H. Maeda, *Adv. Drug Deliv. Rev.* **2011**, *63*, 136–151.
- [21] H. Nakamura, F. Jun, H. Maeda, *Expert Opin. Drug Delivery* **2015**, *12*, 53–64.
- [22] J. Zhang, Z.-F. Yuan, Y. Wang, W.-H. Chen, G.-F. Luo, S.-X. Cheng, R.-X. Zhuo, X.-Z. Zhang, *J. Am. Chem. Soc.* **2013**, *135*, 5068–5073.
- [23] K. Husmann, R. Muff, M. E. Bolander, G. Sarkar, W. Born, B. Fuchs, *Mol. Carcinog.* **2008**, *47*, 66–73.
- [24] G. Bonzi, S. Salmaso, A. Scomparin, A. Eldar-Boock, R. Satchi-Fainaro, P. Caliceti, *Bioconjug. Chem.* **2015**, *26*, 489–501.
- [25] H. Uludag, J. Yang, *Biotechnol. Prog.* **2002**, *18*, 604–611.
- [26] S. Kunjachan, R. Pola, F. Gremse, B. Theek, J. Ehling, D. Moeckel, B. Hermanns-Sachweh, M. Pechar, K. Ulbrich, W. E. Hennink, *Nano Lett.* **2014**, *14*, 972–981.
- [27] D. J. Burkhart, B. T. Kalet, M. P. Coleman, G. C. Post, T. H. Koch, *Mol. Cancer Ther.* **2004**, *3*, 1593–1604.
- [28] W. Jahnke, C. Henry, *ChemMedChem* **2010**, *5*, 770–776.
- [29] S. Zitzmann, V. Ehemann, M. Schwab, *Cancer Res.* **2002**, *62*, 5139–5143.
- [30] Y. Choe, F. Leonetti, D. C. Greenbaum, F. Lecaille, M. Bogyo, D. Brömme, J. A. Ellman, C. S. Craik, *J. Biol. Chem.* **2006**, *281*, 12824–12832.
- [31] S. R. Wilson, C. Peters, P. Saftig, D. Brömme, *J. Biol. Chem.* **2009**, *284*, 2584–2592.
- [32] E. Vlashi, L. E. Kelderhouse, J. E. Sturgis, P. S. Low, *ACS Nano* **2013**, *7*, 8573–8582.
- [33] X. Duan, S.-F. Jia, Z. Zhou, R. R. Langley, M. F. Bolontrade, E. S. Kleinerman, *Clin. Exp. Metastasis* **2005**, *21*, 747–753.
- [34] H. Zhu, H. Cai, M. Tang, J. Tang, *Clin. Transl. Oncol.* **2014**, *16*, 732–738.
- [35] J. D. Lamplot, S. Denduluri, J. Qin, R. Li, X. Liu, H. Zhang, X. Chen, N. Wang, A. Pratt, W. Shui, X. Luo, G. Nan, Z.-L. Deng, J. Luo, R. C. Hydon, T.-C. He, H. H. Luu, *Curr. Cancer Ther. Rev.* **2013**, *9*, 55–77.

Manuscript received: January 11, 2017

Accepted manuscript online: February 22, 2017

Version of record online: March 28, 2017